Zinc Complex of 3,5-di-tert-butyl Salicylate Inhibits the Proliferation, Migration, and Invasion of Triple-Negative Breast Cancer Cells

Heng Chen
Jianghan University
Dong Wang
Jianghan University
Limei Fan
Jianghan University
Weiran Zhang
Jianghan University
Jinhua Xu
Jianghan University
Yunyi Liu (liuyy1987@jhun.edu.cn)
Jianghan University

Research Article

Keywords: TNBC, Zinc complex of 3,5-di-tert-butyl salicylate, Invasion, Migration, JAK-STAT3,RNA-seq

Posted Date: July 29th, 2021

DOI: https://doi.org/10.21203/rs.3.rs-751243/v1

Zinc complex of 3,5-di-tert-butyl salicylate inhibits the Proliferation, Migration, and Invasion of Triple-negative breast cancer cells

Heng Chen, Dong Wang, Limei Fan, Weiran Zhang, Jinhua Xu*, Yunyi Liu*

School of Medicine, Jianghan University, Wuhan, Hubei 430056, China

***Correspondence to:** Jinhua Xu, email: xu5520@gmail.com

Yunyi Liu, email: liuyy1987@jhun.edu.cn

Keywords: *TNBC, Zinc complex of 3,5-di-tert-butyl salicylate, Invasion, Migration, JAK-STAT3,RNA-seq*

Abstract: Zinc complex of 3,5-di-tert-butyl salicylate ($Zn\{[CH_3)_3C]_2Sal\}_2^{2-}$) is a zinc ion chelate of salicylate. In this study, we found that it inhibits the proliferation, invasion, migration and induce apoptosis of triple-negative breast cancer 4T1 cells. The results of RNA-seq showed that expression of 17 genes was up-regulated and 26 genes was down-regulated significantly by $Zn\{[CH_3)_3C]_2Sal\}_2^{2-}$ treatment. Further GO analysis and KEGG analysis showed that the activity of $Zn\{[CH_3)_3C]_2Sal\}_2^{2-}$ against triple-negative breast cancer cells may be involved JAK-STAT3, HIF-1, and TNF signaling pathways. The expression of key genes was verified by RT-PCR. The phosphorylation of STAT3 and its upstream SRC decreased drastically upon $Zn\{[CH_3)_3C]_2Sal\}_2^{2-}$ treatment as analyzed by western blot. Our results indicate that $Zn\{[CH_3)_3C]_2Sal\}_2^{2-}$ inhibits the activity of TNBC cells by down-regulating STAT3 signaling pathway.

Introduction

Breast cancer is the most common cancer among women and accounts for the second largest number of cancer deaths in women worldwide. About 10 to 20 percent of new cases of breast cancer are triple-negative breast cancer (TNBC)[1,2]. TNBC lacks targeted therapies because it does not express estrogen receptor (ER), progesterone receptor (PR) and human epidermal growth factor receptor 2 (HER2)[3]. Compared with other types of breast cancer, TNBC patients have a poor prognosis due to higher risk of metastasis and recurrence[4]. In addition to surgical treatment, chemotherapy is the only FDA approved method for the treatment of TNBC[5]. TNBC is sensitive to chemotherapy in the initial treatment[6], subsequently it become chemotherapy resistant. Therefore, it remains crucial to find the new chemotherapeutic agents in the treatment of TNBC.

Salicylic acids and derivatives are mostly used in antipyretic, analgesic and anti-inflammatory in clinical practice and belong to non-steroidal anti-inflammatory drugs. It also has a certain therapeutic effect on tumors such as breast cancer[7], pancreatic cancer[8], lung cancer[9], ovarian cancer and prostate cancer[10]. It has been found that small doses of aspirin can reduce the risk of multiple cancers, and *in vitro* aspirin inhibits the growth of various

cancer cells including breast cancer through COX-dependent and COX-independent pathway[11]. This inhibition may associate with the salicylic acid group. During the process of breast cancer metastasis, aspirin can resist platelet activation and thus inhibit platelet-induced epithelial transformation, migration and invasion ability of breast cancer cells[12]. Asprin can also inhibit the activation of the transcription factor-1 (AP-1) and the nuclear factor κB (NF-κB), thus affecting cell proliferation, differentiation and apoptosis, transformation, invasion and metastasis of tumor cells[13]. However, there are few studies on the role of heavy metal chelate of salicylate against cancer. Sorenson et al. found that copper salicylate and its derivatives can inhibit the growth and lung metastasis of ascites cancer in animal experiments, induce the differentiation of tumor cells, and thus prolong the survival period of the body[14]. In addition, combined use of copper salicylate can significantly improve the anti-cancer efficacy of cisplatin and reduce its cytotoxicity. O'Connor et al. reported that copper complex of salicylate inhibits the proliferation of MCF-7, DU145, HT29 and SKOV3 cancer cells[15]. Our previous study showed that copper complex of phenanthroline salicylate can induce apoptosis in TNBC cells by down-regulating the expression of anti-apoptosis proteins such as Bcl-2、Bcl-xL and Survivin *in vitro* and *in vivo*[16]. Until now, the function of $Zn\{[CH_3)_3C]_2Sal\}_2^{2-}$ is under investigation.

The activation of signal transduction and transcription (STAT) protein family is closely related to the occurrence and development of many tumors. Among the various STAT members, STAT3 is often over-expressed in tumor cells and tissue samples, and regulates the expression of many oncogenes that control growth and metastasis[17]. As a gathering point of several tumorigenic signaling pathways, STAT3 is considered to have an important role in tumor cells and in the tumor microenvironment. The activation of STAT3 pathways is related to the aggressiveness of breast cancer, and is involved in cell proliferation, apoptosis, metastasis and chemotherapy resistance. Both preclinical and clinical studies have shown that STAT3 plays a crucial role in the progression and metastasis of TNBC[18].

In this study, we investigated the biological effect of $Zn\{[CH_3)_3C]_2Sal\}_2^{2-}$ on TNBC, we found that low concentration of $Zn\{[CH_3)_3C]_2Sal\}_2^{2-}$ could inhibit migration and invasion of TNBC cells. The STAT3 pathway was down regulated by $Zn\{[CH_3)_3C]_2Sal\}_2^{2-}$ treatment as analyzed by RNA-seq and Western Blot. It suggests that $Zn\{[CH_3)_3C]_2Sal\}_2^{2-}$ may play an anti-metastasis of TNBC by inhibiting STAT3 signaling pathway.

Results

Effect of $Zn\{[CH_3)_3C]_2Sal\}_2^{2-}$ on cell proliferation of TNBC cells. $Zn\{[CH_3)_3C]_2Sal\}_2^{2-}$ is a zinc ion chelate of salicylate and its molecular structure was shown in Fig.1A. To examine the effect of $Zn\{[CH_3)_3C]_2Sal\}_2^{2-}$ on TNBC

cell proliferation, TNBC cell 4T1 were incubated with various concentration of $Zn\{[CH_3)_3C]_2Sal\}_2^{2-}$ and then cell viability was measured by MTS assay. As shown in Fig.1B, 4T1 cell viability was not affected by 25 μM $Zn\{[CH_3)_3C]_2Sal\}_2^{2-}$ treatment, however, the viability decreased dramatically by high dose $Zn\{[CH_3)_3C]_2Sal\}_2^{2-}$ treatment. After $Zn\{[CH_3)_3C]_2Sal\}_2^{2-}$ treatment, the IC_{50} of 4T1 cells was 88.459 μM (83.938-92.98), 68.752 μM (64.421-73.082) and 61.784 μM (60.14-63.427) at 24 h, 48 h and 72 h respectively. It suggested that $Zn\{[CH_3)_3C]_2Sal\}_2^{2-}$ inhibits cell proliferation in a time and concentration dependent manner.

Since the viability of TNBC cell was decreased by $Zn\{[CH_3)_3C]_2Sal\}_2^{2-}$,we then analyzed the effects of $Zn\{[CH_3)_3C]_2Sal\}_2^{2-}$ on induction of apoptosis of TNBC cells. 4T1 cells were treated with different concentration of $Zn\{[CH_3)_3C]_2Sal\}_2^{2-}$ for 24 hr and the degree of apoptosis was analysed by Annexin V-PI staining and flow cytometry. As shown in Fig.1C and Fig.1D, less than 5% apoptosis was detected with 25 μM $Zn\{[CH_3)_3C]_2Sal\}_2^{2-}$ treatment. 50 and 100 μM $Zn\{[CH_3)_3C]_2Sal\}_2^{2-}$ treatment could induce apoptosis significantly. It indicates that decreased viability by $Zn\{[CH_3)_3C]_2Sal\}_2^{2-}$ treatment is due to apoptosis induction. It is also suggests that under low concentration(< 25 μM), $Zn\{[CH_3)_3C]_2Sal\}_2^{2-}$ has little effect on cell viability.

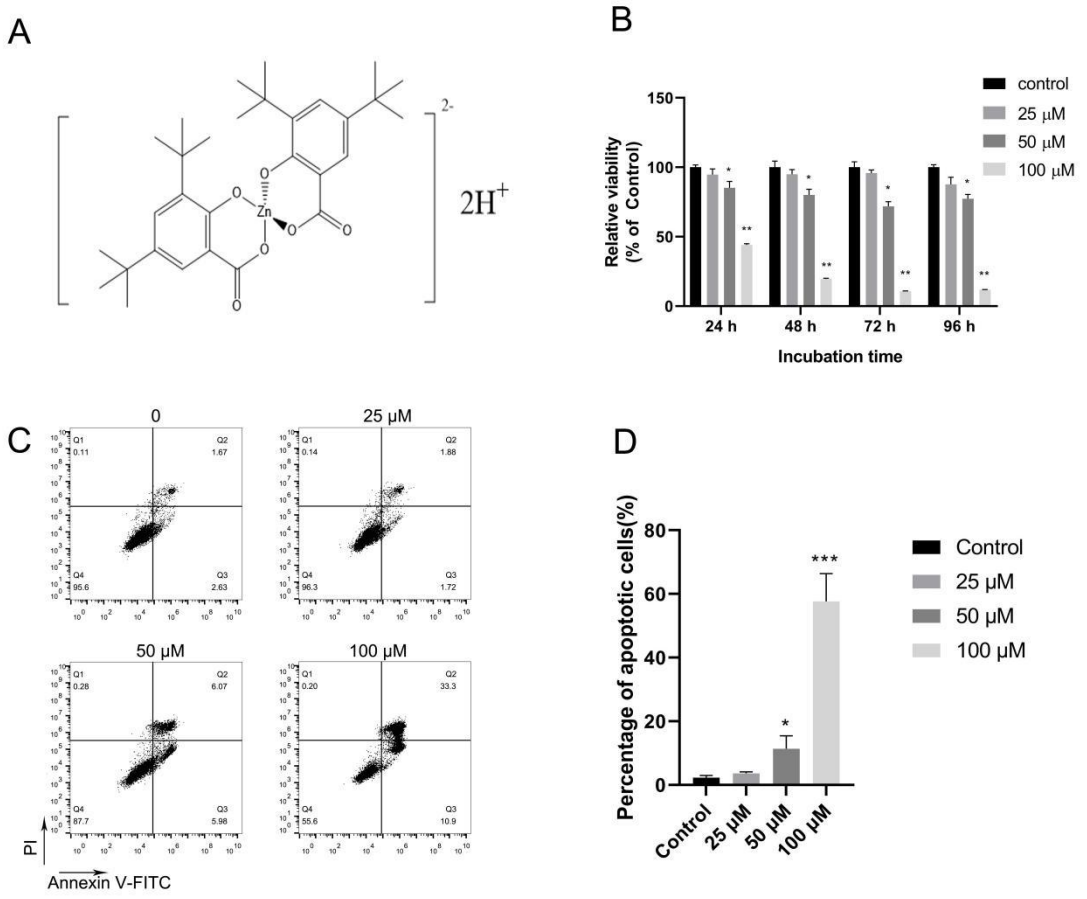

Fig.1 $Zn\{[CH_3)_3C]_2Sal\}_2^{2-}$ inhibits cell proliferation and induces apoptosis of TNBC cells

A) The structure of Zinc complex of 3,5-di-tert-butyl salicylate.

B) Cell viability was decreased by $Zn\{[CH_3)_3C]_2Sal\}_2^{2-}$ treatment. 4T1 cell viability was determined by MTS assay after $Zn\{[CH_3)_3C]_2Sal\}_2^{2-}$ treatments. The statistical analysis was conducted by comparing the OD_{492} value of each treatment concentration with that of DMSO control. Error bars represent mean ± SEM. *P < 0.05, **P < 0.01.
C) $Zn\{[CH_3)_3C]_2Sal\}_2^{2-}$ induced apoptosis of 4T1 cells in a concentration-dependent way. 4T1 cells were incubated with indicated concentrations of $Zn\{[CH_3)_3C]_2Sal\}_2^{2-}$ for 24 hr and apoptosis was measured by flow cytometry after staining with Annexin V-PI staining.
D) Statistical analysis of apoptosis of three independent experiments. Error bars represent mean ± SEM.*P < 0.05, ***P < 0.001.

$Zn\{[CH_3)_3C]_2Sal\}_2^{2-}$ inhibits migration and invasion of 4T1 cells. Since migration is critical for metastasis, we investigated the inhibitory effects of $Zn\{[CH_3)_3C]_2Sal\}_2^{2-}$ on 4T1 cell migration through the wound healing assay. As shown in Fig.2A and Fig.2B, wound healing was hindered by both 10 μM and 25 μM $Zn\{[CH_3)_3C]_2Sal\}_2^{2-}$ treatment compared with the control. The effect was more significant with 25 μM $Zn\{[CH_3)_3C]_2Sal\}_2^{2-}$ treatment. We then investigated whether $Zn\{[CH_3)_3C]_2Sal\}_2^{2-}$ could influence the invasive capacity of 4T1 cells, which is a key step of metastasis. Transwell invasion assays were carried out after 24 hr $Zn\{[CH_3)_3C]_2Sal\}_2^{2-}$ treatment. As shown in Fig.2C and Fig.2D, invasion was reduced by both 10 μM and 25 μM $Zn\{[CH_3)_3C]_2Sal\}_2^{2-}$ treatment compared with the control. The effect was more profound with 25 μM $Zn\{[CH_3)_3C]_2Sal\}_2^{2-}$ treatment. All of these results indicates that $Zn\{[CH_3)_3C]_2Sal\}_2^{2-}$ inhibits migration and invasion of 4T1 cell in a dose-dependent manner.

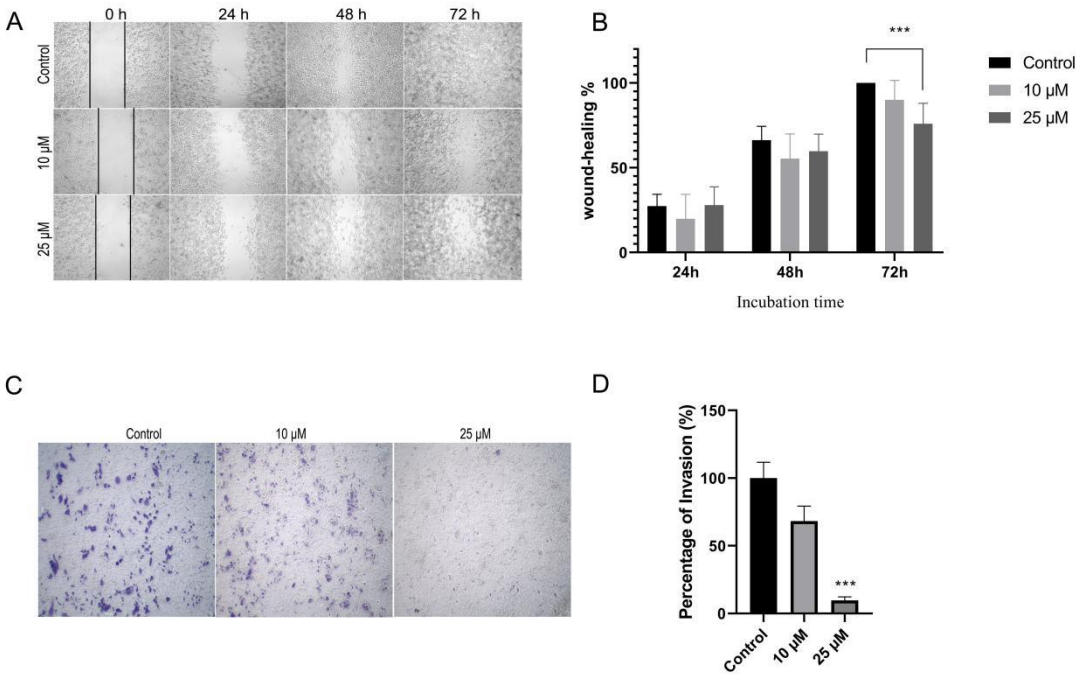

Fig. 2 $Zn\{[CH_3)_3C]_2Sal\}_2^{2-}$ inhibits 4T1 cell migration and invasion.

A) With 10 and 25 μM $Zn\{[CH_3)_3C]_2Sal\}_2^{2-}$ treatment, 4T1cell migration ability was determined by wound healing assay at 0 h, 24 h, 48 h,72h.

B) Statistical analysis of wound healing assay of three independent experiments, Error bars represent mean ± SEM, ***P < 0.001.

C) The invasion ability was determined by a transwell invasion assay after 22 h incubation.

D) Statistical analysis was performed with three independent transwell invasion assays. Error bars represent mean ± SEM. ***P < 0.001.

Gene expression changes in 4T1 cells after $Zn\{[CH_3)_3C]_2Sal\}_2^{2-}$ treatment. To further examine the molecular mechanism of $Zn\{[CH_3)_3C]_2Sal\}_2^{2-}$ against 4T1 cells, RNA-seq analysis was conducted. After $Zn\{[CH_3)_3C]_2Sal\}_2^{2-}$ treatment, expression level of 4965 genes was changed significantly ($p<0.05$). Among those above-mentioned differentially expressed genes, 43 genes have more than 2 time changes, of which 17 genes were up-regulated and 26 genes were down-regulated (Fig.3A&3B).

Enrichment analysis of differentially expressed genes. The Significant Differentially expressed genes (SDEGs) between the control and $Zn\{[CH_3)_3C]_2Sal\}_2^{2-}$ treated 4T1 cells were subjected to functional GO and KEGG pathway analyses. For GO classification, three different categories, including Molecular Function (MF), Cellular Component (CC), and Biological Process (BP), were used to enrich the SDEGs. As shown in Fig.3C, in the MF

category, the SDEGs were primarily enriched in Zinc ion binding, Calcium ion binding, metalloendopeptidase activity, fibronectin binding and MRF binding. In the CC category, they were predominantly enriched in the anchored component of extracellular space and proteinaceous extracellular matrix. In the BP category, they were mainly enriched in terms of response to hypoxia and estradiol, cellular response to interleukin-1, collagen catabolic process and angiogenesis. The top 10 of the 23 enriched KEGG pathways are presented in Fig.3D . Pathways in cancer ranked the highest. Numerous well-established signaling pathways were also enriched, including JAK-STAT signaling pathway, HIF-1 signaling pathway and TNF signaling pathway.

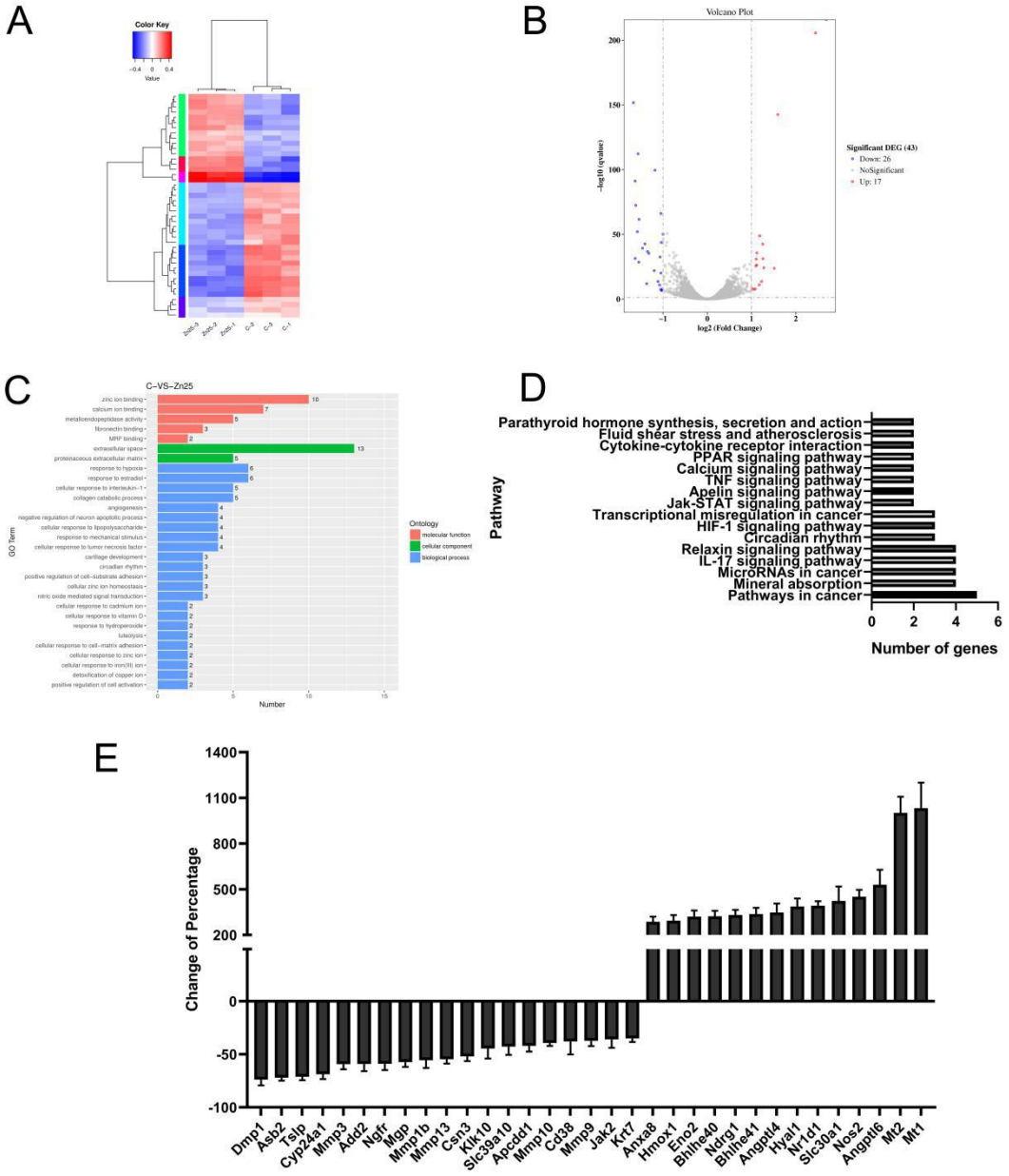

Fig.3 Gene expression changes analyzed by RNA-seq in 4T1 cells after $Zn\{[CH_3)_3C]_2Sal\}_2^{2-}$ treatment

A) Hierarchical clustering of differentially expressed mRNAs between control and $Zn\{[CH_3)_3C]_2Sal\}_2^{2-}$ (25 μM)-treated 4T1 cells.

B) A volcano plot shows differentially expressed RNAs after treating 4T1 cells with $Zn\{[CH_3)_3C]_2Sal\}_2^{2-}$.
C) The enriched cell functional classifications for the DEGs in 4T1cells after treatment with $Zn\{[CH_3)_3C]_2Sal\}_2^{2-}$.
D) The top 16 enriched pathways for the DEGs in 4T1 cells after treatment with $Zn\{[CH_3)_3C]_2Sal\}_2^{2-}$.
E) mRNA expression levels in $Zn\{[CH_3)_3C]_2Sal\}_2^{2-}$-treated 4T1 cells verified by RT-PCR.

Verification of gene expression change by RT-PCR. To confirm the RNA-seq results, expression level of some interesting gene was verified by RT-PCR. As we expected, results of RT-PCR were consistent with RNA-seq analysis. As shown in Fig.3E, the mRNA expression level of MT1 and MT2, which was related Metal ion transportation, were up-regulated nearly 10 times. The expression of Angpt16 and Angp14, which was closely related to angiogenesis, was also significant up-regulated. Meanwhile, Mmp3, Mmp9, Mmp16 and Mmp10, which belong to MMP family and are closely related to tumor metastasis, were down-regulated. Besides that, JAK2, which was an important component of STAT signaling pathway, was down-regulated significantly.

Effects of $Zn\{[CH_3)_3C]_2Sal\}_2^{2-}$ on JAK-STAT signaling pathway, Src pathway and PI3K pathway. JAK-STAT3 signaling pathway is an multiple functional pathway in cancer progress, involving cancer cell proliferation, migration, invasion, and even cancer cell apoptosis. Base on the RNA-seq and RT-PCR results, we believe that JAK-STAT signaling pathway is involved in the anti-cancer effect of $Zn\{[CH_3)_3C]_2Sal\}_2^{2-}$. To test our hypothesis, protein expression and phosphorylation were analyzed in 4T1 cells after $Zn\{[CH_3)_3C]_2Sal\}_2^{2-}$ treatment. As shown in Fig.4A, the expression level of Stat3 and Src protein were not affected by treatment with 25 μM $Zn\{[CH_3)_3C]_2Sal\}_2^{2-}$. However, the phosphorylation of these two proteins was reduced dramatically after 30 min $Zn\{[CH_3)_3C]_2Sal\}_2^{2-}$ treatment. It was still far below the control level after 24hr treatment. These results demonstrated that $Zn\{[CH_3)_3C]_2Sal\}_2^{2-}$ inhibits activation of JAK-STAT3 signaling pathway and Src pathway .Unexpectly, we found that $pAKT^{473}$ was significantly increased after 30min treatment of 25 μM $Zn\{[CH_3)_3C]_2Sal\}_2^{2-}$. To further explore the relationship of $Zn\{[CH_3)_3C]_2Sal\}_2^{2-}$ to AKT, 4T1 cells was treated with 25 μM $Zn\{[CH_3)_3C]_2Sal\}_2^{2-}$ together with AKT inhibitor (MK2206), as shown in Fig.4B, combination treatment suppressed $pAKT^{473}$ completely.

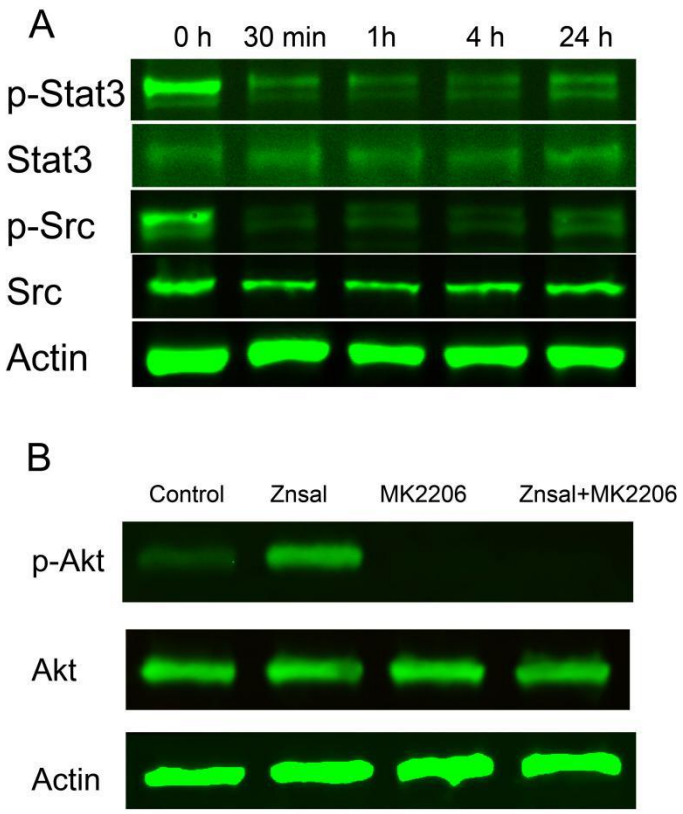

Fig.4 $Zn\{[CH_3)_3C]_2Sal\}_2^{2-}$ inhibits the activation of STAT3 signaling pathway and SRC pathway.

A)The protein expression level of STAT3,p-STAT3,p-Src,Src at different time points in 4T1 cells treated with $Zn\{[CH_3)_3C]_2Sal\}_2^{2-}$ was analyzed by western blot.

B) The protein expression level of Akt and p-Akt as analyzed by western blot after 30min treatment of $Zn\{[CH_3)_3C]_2Sal\}_2^{2-}$, MK2206 alone or combination treatment.

Effect of $Zn\{[CH_3)_3C]_2Sal\}_2^{2-}$ on lung metastasis *in vivo.* Lung metastasis was measured at day 16. As shown in Fig.5, the pulmonary nodules of metastasis in zinc salicylate treatment group and MK2206 treatment group were similar to the control group. In addition, no inhibitory effect on lung metastasis was observed from group treated with $Zn\{[CH_3)_3C]_2Sal\}_2^{2-}$ and MK2206. The weight of $Zn\{[CH_3)_3C]_2Sal\}_2^{2-}$ treated mice decreased slightly

compared with the control group, however, Akt inhibitor MK2206 alone or combination treatment caused weight loss significantly.

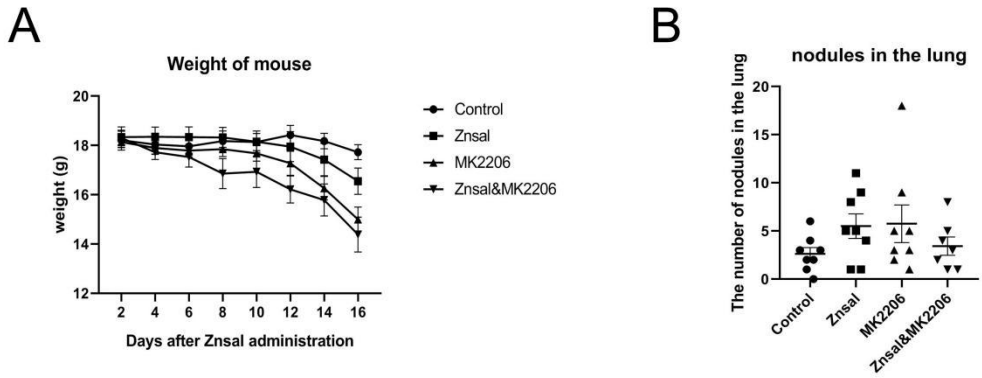

Fig.5 Effect of $Zn\{[CH_3)_3C]_2Sal\}_2^{2-}$ on lung metastasis *in vivo*
Tumorigenesis in the lung of mice was established by injecting 4T1 cells through tail vein of BALB/c mice.
A) Changes in mouse body weight after 16 days treatment of $Zn\{[CH_3)_3C]_2Sal\}_2^{2-}$, MK2206 alone or combination treatment.
B) Number of tumors in the mice lung after 16 days with treatment of $Zn\{[CH_3)_3C]_2Sal\}_2^{2-}$, MK2206 alone or combination treatment.

Discussion

The prognosis of TNBC is poor because of high rate of relapse and metastasis. Drugs that target metastasis are of great significance. In this study, we demonstrated that low dose $Zn\{[CH_3)_3C]_2Sal\}_2^{2-}$ inhibits migration and invasion of mouse TNBC cells 4T1, while high dose $Zn\{[CH_3)_3C]_2Sal\}_2^{2-}$ inhibits cell proliferation and induces apoptosis. In addition, we explored anti-TNBC mechanism of $Zn\{[CH_3)_3C]_2Sal\}_2^{2}$-using RNA-seq and bioinformatic analyses. Furthermore, we demonstrated that $Zn\{[CH_3)_3C]_2Sal\}_2^{2-}$ can inhibit the activation of the STAT3 signaling pathway by western blot analysis.

By utilizing GO and KEGG pathway analyses, We found expression changes of genes associated with Zinc ion binding, metalloendopeptidase activity, fibronectin binding, proteinaceous extracellular matrix, collagen catabolic process and angiogenesis in 4T1 cells. The RT-PCR results verified that the transcription levels of genes related to metal ion transport, angiogenesis, and tumor metastasis have been significantly altered. It indicates that the anti-tumor effect of $Zn\{[CH_3)_3C]_2Sal\}_2^{2-}$ may be related to those genes. In the pathway analyses, many enriched pathways were associated with proliferation, migration, and Invasion, which were consistent with our functional analyses. For instance, JAK-STAT signaling pathway, is important in tumor metastasis. The establishment of a database of RNA expression after $Zn\{[CH_3)_3C]_2Sal\}_2^{2-}$ treatment in 4T1 cell lines could provide a broad foundation to guide focused studies of anti-TNBC research.

The TNBC metastasis mechanism is regulated by multiple signaling pathways,

such as: NF-κB signaling pathway[19], Wnt/beta-Catenin signaling pathway[20], PI3K/AKT signaling pathway, FAK/c-Src pathway[21] and JAK/STAT3 signaling pathway. STAT signaling pathway is the focal point of multiple carcinogenic signaling channels in the body, STAT3 activation is short and strictly controlled, but STAT3 protein appears in contitutively activating in multiple tumor cells[22]. Specifically, Studies have shown that STAT3 affects important processes of tumorigenesis and development of TNBC such as occurrence and metastasis and is highly activated in TNBC[23]. By screening the transcriptional differences between TNBC cells and normal breast cells, Zhan L. et al. and other researchers observed the abnormal expression of multiple signaling proteins of the IL6/JAK2/STAT3 pathway in TNBC, and constitutive activation of JAK2/STAT3 may be an important factor in the distal metastasis of TNBC[24]. Tyrosine kinase SRC also plays an important role in cell proliferation[25], cell cycle, adhesion[26], migration, and invasive signaling pathways, SRC was overexpressed or highly active in various solid tumor cell lines and pathological tissues, and SRC inhibitors inhibited breast cancer cell invasion and metastasis[27]. It has been found that STAT3 are activated by both SRC and JAK2 in breast cancer[22]. Intriguingly, we found $Zn\{[CH_3)_3C]_2Sal\}_2^{2-}$ can inhibit the activation of both SRC and STAT3 and consequently affect migration and invasion ability of 4T1 TNBC cell. This paves the way to develop this chemical as therapeutic drug for TNBC.

We have not detected the anti-metastasis effect of $Zn\{[CH_3)_3C]_2Sal\}_2^{2-}$ in animal work and we condider that the drug was not delivered poperly. Further study with nano-particle delivery is warranted.

Materials and Methods

Materials. $Zn\{[CH_3)_3C]_2Sal\}_2^{2-}$ was synthesized by Dinglong Chemicals (Wuhan, Hubei, China). It was dissolved in dimethyl sulfoxide (DMSO) as stock solution, and further diluted with medium to specific concentrations. Lipofectamine™2000, Roswell Park Memorial Institute (RPMI) 1640 (RPMI-1640), Fetal bovine serum (FBS), and penicillin–streptomycin solution were purchased from Gibco-BRL-Life Technologies (Grand Island, NY). Primers were ordered from Genewiz. Actin, Stat3, Src, phospho-Src, phospho-Akt and Akt antibodies were obtained from Cell Signaling Technology (Danvers, MA, USA). Phospho-Stat3 antibody was purchased from Abcam(Cambridge, UK). 4T1 TNBC cells were obtained from China Center for Type Culture Collection (CCTCC).

MTS assay. To detect the effect of $Zn\{[CH_3)_3C]_2Sal\}_2^{2-}$ on TNBC cell proliferation, cells were plated in 96-well plates and incubated overnight to adhesion, and then treated with different concentrations of $Zn\{[CH_3)_3C]_2Sal\}_2^{2-}$ for indicated time. 20 μl 3-(4,5-dimethylthiazol-2-yl)-5-(3-carboxymethoxyphenyl)-2-(4-sulfophenyl)-2H-tetrazolium (MTS) was added into the culture

medium for 3 h at 37°C. The optical density was read at 490 nm on a microplate reader (Biotek, VT). Quintuplicate wells were measured in each treatment group.

Cell apoptosis detection. Apoptosis of 4T1 cells was determined by Flow cytometry with Annexin V-FITC/PI staining. Cells were plated into six-well plates, after treatment with $Zn\{[CH_3)_3C]_2Sal\}_2^{2-}$ for 24 h, cells were washed with PBS then harvested and further stained according to the manufacturer's instructions. Analysis was performed using flow cytometry (BD Biosciences, San Jose, CA, USA).

Wound Healing Assay. Logarithmic growth phase cells were plated into six-well plates and allow the cells reach 90% confluence. A "scratch" was made by 10 μl pipette tip, and then added different concentration of $Zn\{[CH_3)_3C]_2Sal\}_2^{2-}$. Photograph of the "scratch" fusion was taken in $Zn\{[CH_3)_3C]_2Sal\}_2^{2-}$ treated group and the control group each 12 h. Image J software was used for Image data analysis.

Cell Invasion Assay. Transwell chambers with matrigel-coated membranes were placed in 24-well plates and incubated with 500 ul serum free medium at 37°C for 2 hr. Then, 4T1 cells (1×10^5) in 500 μl of serum-free medium were seeded into the top chamber and 750 μl of RPMI-1640 medium with 10% FBS were added into the down compartment of the transwell chambers as the chemical attractant. After incubation for 22 hr at 37°C, the cells were fixed and stained with crystal violet. The invaded cells in five randomly chosen fields of each well were counted.

RNA-sequencing. The cDNA library construction, library purification and transcriptome sequencing were carried out according to the Suzhou GENEWIZ Company's instructions. Three samples were used in each group for RNA- sequencing assay.

GO and KEGG Pathway Enrichment Analysis. Differential expression analysis used the DESeq2 Bioconductor package, a model based on the negative binomial distribution. the estimates of dispersion and logarithmic fold changes incorporate data-driven prior distributions, Padj of genes were setted <0.05 to detect differentially expressed ones. GOSeq (v1.34.1) was used identifying Gene Ontology (GO) terms that annotate a list of enriched genes with a significant padj less than 0.05. And top GO was used to plot DAG. KEGG (Kyoto Encyclopedia of Genes and Genomes) is a collection of databases dealing with genomes, biological pathways, diseases, drugs, and chemical substances (http://en.wikipedia.org/wiki/KEGG). We used scripts in

house to enrich significant differential expression gene in KEGG pathways.

RNA extraction and Quantitative Real-time RT-PCR. Total RNA was extracted from 4T1 cells using TRIZOL reagent (Invitrogen, Carlsbad, CA, USA) to analyze differentially expressed gene. cDNA was prepared from 1 μg of total RNA using SuperScript® III First-Strand Synthesis System kit (Invitrogen) according to the manufacturer's instructions. Quantitative real-time polymerase chain reaction (qRT-PCR) was carried out in CFX Connect™ Real-time System (Bio-rad,Singapore) using iTaq Universal SYBR Green Supermix (Hercules, CA, USA). Primers used in this study are listed in Supplemental Table S1. The $2^{(-\Delta\Delta Ct)}$ method was used to analyze relative expression changes of mRNA and β-actin was used as internal reference.

Western blotting assay. After treated with different concentrations of $Zn\{[CH_3)_3C]_2Sal\}_2^{2-}$ or MK2206（AKT inhibitor）for a specific period of time, the cell protein was extracted according to the experimental instructions, separated by SDS-PAGE, transferred to the nitrocellulose filter membrane (Pall, Pensacola, USA).The membranes were incubated with the specific primary antibody, and then incubated with the with IRDye secondary antibodies (Licor, NB, USA). The membranes were scanned and the images were captured with Odyssey SA (Licor, NB, USA).

Animal model for lung metastasis. Animal experiments were approved by the ethics committee of Jianghan University and in accordance with relevant guidelines and regulations including ARRIVE guidelines. The experimental mice were purchased from Wuhan Wanqian Jiaxing Biotechnology Co., Ltd. 4T1 cells ($5x10^4$ cells in 100 μl volume) were injected through tail vein of 6-week-old female BALB/c mice. $Zn\{[CH_3)_3C]_2Sal\}_2^{2-}$(15mg/kg) was administered by intraperitoneal injection three times a week after transplantation. For AKT inhibitor, mice were gavaged with 0.1mL MK2206 (120mg/kg) three times a week. Combination treatment was done accordingly. Animals were humanely sacrificed on day 16 after 4T1 transplantation, and the number of tumor nodules in lungs was recorded for analysis of metastasis.

Statistical Analysis. All statistical analyses were performed using GraphPad Prism 8 software (GraphPad Software, Inc., La Jolla, CA, USA). Comparison between two groups was performed using Student's t-test. Statistical significance was defined as * $p < 0.05$ and ** $p < 0.01$.Data were expressed as the mean ± standard deviation, $n \geq 3$,unless otherwise stated.

Acknowledgements

This work was financially supported by the grant from the Natural Science Foundation of China (81602642) to Y. Liu., Huanghe Talented Scholar Grant of Wuhan City to J. Xu (1010/06850002), Jianghan University collaborative Innovation grant (3010/03100070) to J.Xu., Jianghan University Talent Training Grant (3015/06210046) to Y.Liu. J. Xu is a Chutian Scholar of Department of Education, Hubei Province.

Author contributions

Y.Liu., R.Zhang and J.Xu conceived and designed the experiments. H.Chen, D.Wang. and M.Fan performed the experiments. H.Chen and Y.Liu analyzed the data. Y.Liu and J.Xu wrote the paper. All authors reviewed the manuscript.

Competing interests

The authors declare no competing interests.

References

1 Jauhari, Y. *et al.* The influence of age, comorbidity and frailty on treatment with surgery and systemic therapy in older women with operable triple negative breast cancer (TNBC) in England: A population-based cohort study. *Eur J Surg Oncol* **47**, 251-260, https://doi.org/10.1016/j.ejso.2020.09.022 (2021).

2 Jenie, R. I. *et al.* The Evaluation of Cytotoxic Properties from CCB-2 Sugar Complexes Against TNBC and Non-TNBC Cells. *Asian Pac J Cancer Prev* **22**, 151-155, https://doi.org/10.31557/APJCP.2021.22.1.151 (2021).

3 Killock, D. Pembrolizumab can delay progression of TNBC. *Nat Rev Clin Oncol* **18**, 1817-1828, https://doi.org/10.1038/s41571-020-00465-x (2021).

4 Moreira, M. P., Braga, L. D., Cassali, G. D. & Silva, L. M. STAT3 as a promising chemoresistance biomarker associated with the CD44(+/high)/CD24(-/low)/ALDH(+) BCSCs-like subset of the triple-negative breast cancer (TNBC) cell line. *Experimental Cell Research* **363**, 283-290, https://doi.org/10.1016/j.yexcr.2018.01.018 (2018).

5 Jin, J., Tao, Z., Cao, J., Li, T. & Hu, X. DNA damage response inhibitors: An avenue for TNBC treatment. *Biochim Biophys Acta Rev Cancer* **1875**, 188521, https://doi.org/10.1016/j.bbcan.2021.188521 (2021).

6 Vagia, E., Mahalingam, D. & Cristofanilli, M. The Landscape of Targeted Therapies in TNBC. *Cancers (Basel)* **12**, 916-941, https://doi.org/10.3390/cancers12040916 (2020).

7 Karalis, T. T. *et al.* Salicylate suppresses the oncogenic hyaluronan network in metastatic breast cancer cells. *Matrix Biol Plus* **6-7**, 100031, https://doi.org/10.1016/j.mbplus.2020.100031 (2020).

8 Tran, P. O., Gleason, C. E. & Robertson, R. P. Inhibition of interleukin-1beta-induced COX-2 and EP3 gene expression by sodium salicylate enhances pancreatic islet beta-cell function. *Diabetes* **51**, 1772-1778, https://doi.org/10.2337/diabetes.51.6.1772 (2002).

9 O'Brien, A. J. *et al.* Salicylate activates AMPK and synergizes with metformin to reduce the survival of prostate and lung cancer cells ex vivo through inhibition of de novo lipogenesis. *Biochem J* **469**, 177-187, https://doi.org/10.1042/BJ20150122 (2015).

10 Gnanaprakasam, J. N. R., Lopez-Banuelos, L. & Vega, L. Anacardic 6-pentadecyl salicylic acid induces apoptosis in breast cancer tumor cells, immunostimulation in the host and decreases blood toxic effects of taxol in an animal model. *Toxicol Appl Pharmacol* **410**, 115359, https://doi.org/10.1016/j.taap.2020.115359 (2021).

11 Shtivelband, M. I., Juneja, H. S., Lee, S. & Wu, K. K. Aspirin and salicylate inhibit colon cancer medium- and VEGF-induced endothelial tube formation: correlation with suppression of cyclooxygenase-2 expression. *J Thromb Haemost* **1**, 2225-2233, https://doi.org/10.1046/j.1538-7836.2003.00446.x (2003).

12 Madunic, J. *et al.* Sodium Salicylate Inhibits Urokinase Activity in MDA MB-231 Breast Cancer Cells. *Clin Breast Cancer* **17**, 629-637, https://doi.org/10.1016/j.clbc.2017.03.015 (2017).

13 Lin, L., Li, G., Zhang, W., Wang, Y. L. & Yang, H. Low-dose aspirin reduces hypoxia-induced sFlt1 release via the JNK/AP-1 pathway in human trophoblast and endothelial cells. *J Cell Physiol* **234**, 18928-18941, https://doi.org/10.1002/jcp.28533 (2019).

14 Sorenson, J. R. & Wangila, G. W. Co-treatment with copper compounds dramatically decreases toxicities observed with cisplatin cancer therapy and the anticancer efficacy of some copper chelates supports the conclusion that copper chelate therapy may be markedly more effective and less toxic than cisplatin therapy. *Curr Med Chem* **14**, 1499-1503, https://doi.org/10.2174/092986707780831041 (2007).

15 O'Connor, M. *et al.* Copper(II) complexes of salicylic acid combining superoxide dismutase mimetic properties with DNA binding and cleaving capabilities display promising chemotherapeutic potential with fast acting in vitro cytotoxicity against cisplatin sensitive and resistant cancer cell lines. *J Med Chem* **55**, 1957-1968, https://doi.org/10.1021/jm201041d (2012).

16 Fan, L. *et al.* Salicylate *Phenanthroline copper (II) complex induces apoptosis in triple-negative breast cancer cells. *Oncotarget* **8**, 29823-29832, https://doi.org/10.18632/oncotarget.16161 (2017).

17 Chong, P. S. Y., Chng, W. J. & de Mel, S. STAT3: A Promising Therapeutic Target in Multiple Myeloma. *Cancers* **11**, https://doi.org/ARTN 73110.3390/cancers11050731 (2019).

18 Dai, X. X. *et al.* Osthole inhibits triple negative breast cancer cells by suppressing STAT3. *J Exp Clin Canc Res* **37**, https://doi.org/ARTN 32210.1186/s13046-018-0992-z (2018).

19 Wang, P. *et al.* Ginsenoside panaxatriol reverses TNBC paclitaxel resistance by inhibiting the IRAK1/NF-kappaB and ERK pathways. *PeerJ* **8**, e9281, https://doi.org/10.7717/peerj.9281 (2020).

20 Xu, J., Koval, A. & Katanaev, V. L. Beyond TNBC: Repositioning of Clofazimine Against a Broad Range of Wnt-Dependent Cancers. *Front Oncol* **10**, 602817, https://doi.org/10.3389/fonc.2020.602817 (2020).

21 Rigiracciolo, D. C. *et al.* Correction: Rigiracciolo, D.C., et al., IGF-1/IGF-1R/FAK/YAP Transduction Signaling Prompts Growth Effects in Triple-Negative Breast Cancer (TNBC) Cells. Cells 2020, 9, 1010. *Cells* **9**, https://doi.org/10.3390/cells9122619 (2020).

22 Garcia, R. *et al.* Constitutive activation of Stat3 by the Src and JAK tyrosine kinases participates in growth regulation of human breast carcinoma cells. *Oncogene* **20**, 2499-2513, https://doi.org/10.1038/sj.onc.1204349 (2001).

23 Jackson, J. G. & Lozano, G. TNBC invasion: downstream of STAT3. *Oncotarget* **8**, 20517-20518, https://doi.org/10.18632/oncotarget.15259 (2017).

24 Kim, M. S., Lee, W. S., Jeong, J., Kim, S. J. & Jin, W. Induction of metastatic potential by TrkB via activation of IL6/JAK2/STAT3 and PI3K/AKT signaling in breast cancer. *Oncotarget* **6**, 40158-40171, https://doi.org/10.18632/oncotarget.5522 (2015).

25 Nishida, H. *et al.* Methionine restriction breaks obligatory coupling of cell proliferation and death by an oncogene Src in Drosophila. *Elife* **10**, https://doi.org/10.7554/eLife.59809 (2021).

26 Chatterjee, T. *et al.* Anti-GPR56 monoclonal antibody potentiates GPR56-mediated Src-Fak signaling to modulate cell adhesion. *J Biol Chem* **296**, 100261, https://doi.org/10.1016/j.jbc.2021.100261 (2021).

27 Proietti, C. *et al.* Progestins induce transcriptional activation of signal transducer and activator of transcription 3 (Stat3) via a Jak- and Src-dependent mechanism in breast cancer cells. *Mol Cell Biol* **25**, 4826-4840, https://doi.org/10.1128/MCB.25.12.4826-4840.2005 (2005).

Supplementary Files

This is a list of supplementary files associated with this preprint. Click to download.

- SupplementaltableS1.pdf